**JCRT.ORG** 

ISSN: 2320-2882



## INTERNATIONAL JOURNAL OF CREATIVE **RESEARCH THOUGHTS (IJCRT)**

An International Open Access, Peer-reviewed, Refereed Journal

# **Modeling And Control Of Three-Phase Active** Front End Rectifier Using Decoupled Dq Control

<sup>1</sup>Abdirahman Omar Hassan, <sup>2</sup>Dr.R. Srinu Naik, <sup>3</sup>S. Naveena,

<sup>1</sup>PG Scholar, <sup>2</sup>Associate Professor, <sup>3</sup>Research Scholar

<sup>1</sup>Department of Electrical Engg., Andhra University College of Engineering(A), Andhra University, Visakhapatnam, India.

#### Abstract

Due to low harmonic distortion of the line current, bi-directional power flow and unity power factor feature offered by Insulated Gate Bipolar Transistor (IGBT) based active front-end converters are widely used in industrial applications which served as additional benefits. This paper conducts a comprehensive study on the modeling and control of a three-phase active front-end rectifier system with decoupled dq based control strategy. The operational details of the active front-end converter system are investigated, along with considerations regarding controller design to enhance disturbance rejection and robustness. Experimental validation demonstrates the effectiveness of the proposed control method on improving system performance in different operational circumstances.

Keywords: Three-Phase Rectifier, Active Front End (AFE), Decoupled dq Control, MATLAB Simulation.

#### Introduction:

Power electronic systems that are dependable and efficient are becoming more and more necessary in modern industrial applications. In this context, active front-end rectifiers have become essential elements, acting as a link between the grid and different loads, including motor drives [1], energy storage systems [2], renewable energy systems [3] and HEV battery chargers [4].

Three-phase rectifiers, in particular, are widely employed due to their ability to handle higher power levels compared to single-phase counterparts. By utilizing multilevel topologies, these rectifiers offer advantages [5] such as better power quality, smaller passive filters, less voltage stress on semiconductors, lower common-mode voltages, and higher conversion efficiency.

Pair of two feedback loops is usually used to control these rectifiers: the outside DC-link voltage loop and the inside current loop. Typically, an L filter [6-10] is used to link these rectifiers to the grid in order to simplify the method of control design. Nevertheless, the L filter is unable to effectively reduce grid current harmonics when its inductance is low. There are two main approaches that can be used to solve this problem and attain the required degree of grid current harmonic filtering. The first approach, however, increases the switching frequency at the expense of higher system losses. The second approach uses a greater inductance, which reduces harmonics effectively

but causes a huge voltage drop, which impairs the entire system's performance.

LCL filters, which offer better attenuation than L filters, are thought to be a useful remedy for grid-connected rectifiers [11-20] in order to overcome this problem. However, because an LCL filter is third-order and requires efficient resonance damping, using one raises control complexity. There are two main ways to produce resonance damping. The first technique, known as passive damping, is attaching a tiny resistor inside the LCL filter [22]. This approach increases system losses and is therefore not favored even though it can produce the desired dampening effect. As opposed to using a physical resistor in the LCL filter, the second technique, known as active damping, makes use of a virtual resistor inside the control scheme. Although efficient, this approach might need further measurements on top of the ones already included in the control strategy, including LCL filter currents and voltages, depending on where the virtual resistor is placed.

On the contrary, a variety of control strategies have been developed for three-phase rectifiers with LCL filters in order to achieve control goals like maximizing power factor operation, offering a quick dynamic response to unexpected load and reference changes, and reducing total harmonic distortion (THD) in grid currents. Measurements of grid current [11], rectifier current [12-15], both grid

current and rectifier current [16], and rectifier current and capacitor current and more other needed measurements (i.e. capacitor voltage measurements [17], rectifier current and capacitor voltage measurements [18, 19], and grid current and capacitor current measurements [20, 21]) are required by these methods. One can comprehend how complicated of these control techniques by taking into account the quantity of measures that are necessary. The expenses and power losses associated with the measurements rise with the number of sensors, and the increased likelihood of sensor failures negatively impacts system reliability. Since measurement mistakes are a recognized inherent feature of real-time implementations.

The heart of an active front-end rectifier lies in its control system, which governs the operation of the power electronic devices to achieve desired performance objectives. Recent studies have suggested a number of control schemes for three-phase active front-end (AFE) rectifiers. The performance, efficiency, and stability of the system are to be improved by these methods. Current sensor-less solutions, such as those based on mathematical models [23] [24], that get rid of the necessity for current measurements are examples of control approaches. Furthermore, with an emphasis on high-power applications like the infrastructure for charging electric vehicles (EVs), techniques like Voltage Orientated Control (VOC), Direct Power Control (DPC), Hysteresis Current Control (HCC), and Model Predictive Control (MPC) have been applied and compared in AFE rectifiers [25]. Management techniques for single-phase AFE rectifiers have also been created to deal with problems such as dc-bus voltage fluctuations and ac-side current quality, using Deadbeat Predictive (DP) controllers for grid voltage management and PI controllers for grid current control [26]. By optimizing system performance under diverse operating conditions, these solutions seek to guarantee the dependable and effective functioning of AFE rectifiers. Decoupled dq control is one such methodology that has gained popularity in recent years due to its simplicity and effectiveness in regulating active and reactive power independently. This control technique refers to a control strategy that aims to achieve independence between the direct (d) and quadrature (q) components of control signals.

In this research, we study the decoupled dq control methodology for modeling and controlling a three-phase active front-end rectifier system. Decoupled dq control improves system performance and efficiency by precisely regulating active and reactive power by separating the control variables into direct and quadrature axes. We examine the working principles of the active front-end converter system using MATLAB simulation, and we assess whether decoupled dq control is effective in achieving the best possible performance in a range of operating scenarios.

The remainder of this paper is structured as follows: Section 2 provides a comprehensive review control

method. Section 3 details the mathematical model employed in the design and simulation of the active frontend rectifier system, Section 4 presents the dq control in details including the overall block diagram, Section 5 presents the simulation setup and simulation results found during the execution of the system build in Matlab Simulink, followed by a conclusion and discussion in Section 6, which interprets the findings and assesses the performance of the proposed control technique and summarizing the key findings and suggesting avenues for future research.

#### **Review of Control Method**

The dq control theory is fundamental in power electronics for simplifying the control of threephase AC systems. This theory involves transforming the three-phase quantities into two orthogonal components (d and q axes) in a rotating reference frame. The primary advantage of this transformation is that it converts AC quantities, which are time-varying, into DC quantities that are easier to manage with standard control techniques such as PI controllers.

The transformation from the three-phase abc frame to the dq0 frame (also known as Park's transformation) is given by the following equations:

$$\begin{bmatrix} d \\ q \\ 0 \end{bmatrix} = \frac{2}{3} \begin{bmatrix} \cos(\theta) & \cos\left(\theta - \frac{2\pi}{3}\right) & \cos\left(\theta + \frac{2\pi}{3}\right) \\ \sin(\theta) & \sin\left(\theta - \frac{2\pi}{3}\right) & \sin\left(\theta + \frac{2\pi}{3}\right) \\ \frac{1}{2} & \frac{1}{2} & \frac{1}{2} \end{bmatrix} \begin{bmatrix} a \\ b \\ c \end{bmatrix}$$
 (1)

Here,  $\theta$  is the angular position of the rotating reference frame, and a, b, c is the three-phase quantities. This transformation reduces the complexity of controlling AC signals by converting them into two DC-like signals (d and q components) and one zero-sequence component, which is typically zero for balanced systems.

#### Where:

 $\theta$  is the angular position of the rotating reference

a, b, c are the three-phase quantities.

d, q are the direct and quadrature axis components in the rotating reference frame.

The inverse transformation, which converts the dq0 components back to the abc frame, is given

by:
$$\begin{bmatrix}
a \\ b \\
c
\end{bmatrix} = \begin{bmatrix}
\cos(\theta) & \sin(\theta) & 1 \\
\cos(\theta - \frac{2\pi}{3}) & \sin(\theta - \frac{2\pi}{3}) & 1 \\
\cos(\theta + \frac{2\pi}{3}) & \sin(\theta + \frac{2\pi}{3}) & 1
\end{bmatrix} \begin{bmatrix}
d \\ q \\
0
\end{bmatrix} (2)$$
From (1) the Park transformation is given by:

From (1) the Park transformation is given by:

$$\begin{pmatrix} id \\ iq \\ io \end{pmatrix} = \frac{2}{3} \begin{pmatrix} \cos\theta & \cos\left(\theta - \frac{2\pi}{3}\right) & \cos\left(\theta + \frac{2\pi}{3}\right) \\ -\sin\theta & -\sin\left(\theta - \frac{2\pi}{3}\right) & -\sin\left(\theta + \frac{2\pi}{3}\right) \\ \frac{1}{2} & \frac{1}{2} & \frac{1}{2} \end{pmatrix} \begin{pmatrix} ia \\ ib \\ ic \end{pmatrix}$$
 (3)

Where id and iq are the direct and quadrature components of the current, respectively, and  $\theta$  is the angular position of the rotating reference frame.

Regulating id in order to control the DC bus voltage and iq in order to regulate reactive power is how the Active Front End (AFE) rectifier is controlled in the dq reference frame. The control architecture is made simpler by decoupling the dq components, which makes it possible to independently tune the active and reactive power control loops. This technique improves the dynamic performance and stability of the rectifier by enabling precise control over its output.

The outer voltage control loop and the inner current control loop are the two main loops that typically make up the control structure. Through the creation of a reference current for the inner loop, the outer loop regulates the DC bus voltage. After that, the inner loop makes sure the reference and real current match, resulting in the required performance. In both loops, proportional-integral (PI) controllers are usually employed to preserve stability and offer a quick dynamic response.

#### 3 **Mathematical model**

The modeling of the three-phase active front end rectifier involves representing the system with differential equations that describe the electrical characteristics of the rectifier in both the abc and dq frames.

System Equations in abc Frame:

The dynamic behavior of a three-phase active front end rectifier can be described using the following set of differential equations:

$$\begin{cases} van=L\frac{dia}{dt} + Ria+Vao \\ vbn=L\frac{dib}{dt} + Rib+Vbo \\ vcn=L\frac{dic}{dt} + Ric+Vco \end{cases}$$
 (4)

#### Here:

van, vbn, vcn are the phase voltages.

ia, ib, ic are the phase currents.

L and R represent the inductance and resistance of the rectifier circuit.

vao, vbo, vco are the voltages at the output of the converter.

Transformation to dq Frame:

Using the dq transformation, these equations (4) are transformed into the dq reference frame, which simplifies the control strategy. The transformed equations are:

$$\begin{cases} vd=L\frac{did}{dt}-wLiq+Rid+vdo\\ vq=L\frac{diq}{dt}-wLid+Riq+vqo \end{cases} \tag{5}$$

vd, vq are the d and q axis voltages.

id, iq are the d and q axis currents.

 $\omega$  is the angular frequency of the rotating reference frame.

vdo, vgo are the d and q axis components of the output voltage.

#### State Space Representation:

The state-space representation provides a compact form for modeling and control design. The state variables are the currents id and iq, and the statespace equations are derived from the differential equations starting from equations (5).

$$\begin{cases} vd = L \frac{did}{dt} - wLiq + Rid + vdo \\ vq = L \frac{diq}{dt} - wLid + Riq + vqo \end{cases}$$
 (6)

The state vector x and the input vector u are defined as:

$$\frac{\mathbf{d}}{\mathbf{dt}} \begin{bmatrix} i \mathbf{d} \\ i \mathbf{q} \end{bmatrix} = \begin{bmatrix} \frac{R}{L} & \mathbf{w} \\ -\mathbf{w} & -\frac{R}{L} \end{bmatrix} \begin{bmatrix} i \mathbf{d} \\ i \mathbf{q} \end{bmatrix} + \begin{bmatrix} \frac{1}{L} & 0 \\ 0 & \frac{1}{L} \end{bmatrix} \begin{bmatrix} v \mathbf{d} \\ v \mathbf{q} \end{bmatrix}$$
(7)

Or in a compact form:

$$\dot{\mathbf{x}}$$
= $\mathbf{A}\mathbf{x}$ + $\mathbf{B}\mathbf{u}$  (8) Where:

$$A = \begin{bmatrix} -\frac{R}{L} & w \\ -\frac{R}{V} & -\frac{R}{L} \end{bmatrix}, \qquad B = \begin{bmatrix} \frac{1}{L} & 0 \\ 0 & \frac{1}{L} \end{bmatrix}$$
(9)

## Decoupled dq Control Strategy:

The decoupled dq control strategy aims to independently control the direct (d) and quadrature (q) axis components to achieve desired performance criteria such as voltage regulation and power factor correction. This involves designing PI controllers for each axis using equations (5) we get:

Vd,ref=Kpd( id,ref-id)+ Kid 
$$\int$$
 (id,ref-id)dt (10)  
Vq,ref=Kpq( iq,ref-iq)+ Kiq  $\int$  (iq,ref-iq)dt (11)

Where:

Vd,ref, Vq,ref are the reference voltages for the d

id,ref, iq,ref are the reference currents for the d and q axes.

Kpd, Kpq are the proportional gains for the d and

Kid, Kiq are the integral gains for the d and q axes.

These PI controllers adjust the output to ensure that the system operates according to the desired set points, which makes possible in achieving effective decoupled control of the rectifier.

#### **Assumptions:**

To simplify the modeling process, several assumptions are made:

Balanced System Operation: The three-phase system is assumed to be balanced, meaning that the three-phase voltages and currents are symmetrical and have equal magnitudes.

Ideal Switching: The power electronic switches in the rectifier are assumed to operate ideally, with instantaneous switching and no power losses.

Negligible: Parasitic elements such as stray inductances and capacitances are considered negligible and do not significantly affect the system dynamics.

Constant Parameters: The inductance L and resistance R of the input filter are considered constant and do not vary with operating conditions.

These assumptions help in developing simplified yet accurate model of the three-phase active front end rectifier, making it easier to design and implement the control strategy.

#### **Control Strategy implementation**

#### 4.1 concept of dq control:

Decoupled dq control in power electronics is important to be able to manage three-phase AC systems. By transforming the three-phase currents and voltages to dq reference frame, it is possible to control more easily sinusoidal signal as in case of Field Oriented Control or DC-like signals. This transformation allows to control the d and q components of the system's direct (d) and quadrature (q) axis, this empowers exact control over active power reactive The dynamic equations of the system are decoupled into two separate control loops in the dq frame. Generally speaking, the d-axis regulates the direct voltage or active power, and the q-axis regulates the reactive voltage or quadrature voltage. With each axis controlled independently, this decoupling enables the use of common controllers such as proportional-integral (PI) controllers for more straightforward and efficient control techniques.

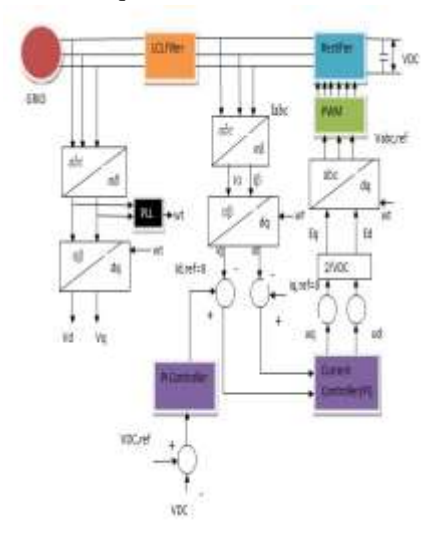


Fig. 1 The Overall Block diagram of system

#### 4.2 control implementation details

The control algorithm for decoupled dq control involves the following steps:

Measurement and Transformation: Measure the three-phase currents and voltages. Transform these measurements from the abc frame to the dq frame using the Park transformation.

$$\begin{bmatrix} \mathbf{d} \\ \mathbf{q} \\ 0 \end{bmatrix} = \frac{2}{3} \begin{bmatrix} \cos(\theta) & \cos\left(\theta - \frac{2\pi}{3}\right) & \cos\left(\theta + \frac{2\pi}{3}\right) \\ \sin(\theta) & \sin\left(\theta - \frac{2\pi}{3}\right) & \sin\left(\theta + \frac{2\pi}{3}\right) \end{bmatrix}$$

$$\begin{bmatrix} \mathbf{d} \\ \frac{1}{2} & \frac{1}{2} & \frac{1}{2} \end{bmatrix}$$

Error Calculation: Calculate the error between the reference and actual values for both the d and q axes.

$$eq=iq,ref-iq$$
 (14)

PI Control: Apply PI controllers to the d and q axis errors to compute the control voltages.

Vd,ref=Kpd ed+Kid 
$$\int$$
 ed dt (15)

$$Vq,ref=Kpq eq+Kiq \int eq dt$$
 (16)

Decoupling and Compensation: Compensate for the cross-coupling terms due to the rotating reference frame.

$$Vd=Vd,ref+wLiq$$
 (17)

$$Vq=Vq,ref+wLid$$
 (18)

Inverse Transformation: Transform control voltages back to the abc frame using the inverse Park transformation.

$$\begin{bmatrix} a \\ b \\ c \end{bmatrix} = \begin{bmatrix} \cos(\theta) & \sin(\theta) & 1 \\ \cos(\theta - \frac{2\pi}{3}) & \sin(\theta - \frac{2\pi}{3}) & 1 \\ \cos(\theta + \frac{2\pi}{3}) & \sin(\theta + \frac{2\pi}{3}) & 1 \end{bmatrix}$$

$$\begin{bmatrix} d \\ q \\ 0 \end{bmatrix}, \qquad (15)$$

PWM Generation: Use the transformed voltages to generate PWM signals for the inverter switches.

#### 5 **Simulation setup**

The testing and simulation of the 3-phase active rectifier (front-end converter) is outlined in this section. The simulation is conducted using MATLAB/Simulink, The main aim is to analyze the performance of this active rectifier at different operating conditions.

#### **Converter Specifications:**

Rated Power: 100 kW

DC Voltage: 800 V Grid Voltage: 415 V RMS (line-to-line)

Grid Frequency: 50 Hz

Switching Frequency: 10 kHz

### **Simulation Configuration:**

- **MATLAB/Simulink Environment: The** MATLAB/Simulink environment, which offers an extensive toolkit for modeling, simulating, and analyzing dynamic systems, is where the simulation is configured. Electrical components are modeled using the Power System Block set, while control algorithm design and tuning are facilitated using the Control System Toolbox.
- Grid Configuration: The active rectifier is connected to a three-phase grid with a line-to-line RMS voltage of 415 V and a frequency of 50 Hz. The grid is modeled to provide a stable and consistent supply, simulating real-world operating conditions.
- LCL filter design: The LCL filter components (L1, C, L2) are selected to provide optimal harmonic attenuation. The design criteria include selecting appropriate inductance and capacitance values to achieve a balance between filtering effectiveness and system stability.
- \* Rectifier Design: The three-phase bridge rectifier uses IGBTs, which are controlled using Pulse Width Modulation (PWM) with a switching frequency of 10 kHz. The high switching frequency ensures that the inverter operates efficiently, with minimal harmonic distortion in the output waveform.

Control Strategy: The decoupled dq control strategy is implemented to regulate the active and reactive power independently. PI controllers designed and tuned for the d and q axes to ensure accurate and stable operation. The control algorithm is coded in MATLAB and integrated into the Simulink model.

#### **Simulation Results:**

The system is been designed and simulated as per in figure 2, and the description of the above section is been followed to execute the system and get the results.

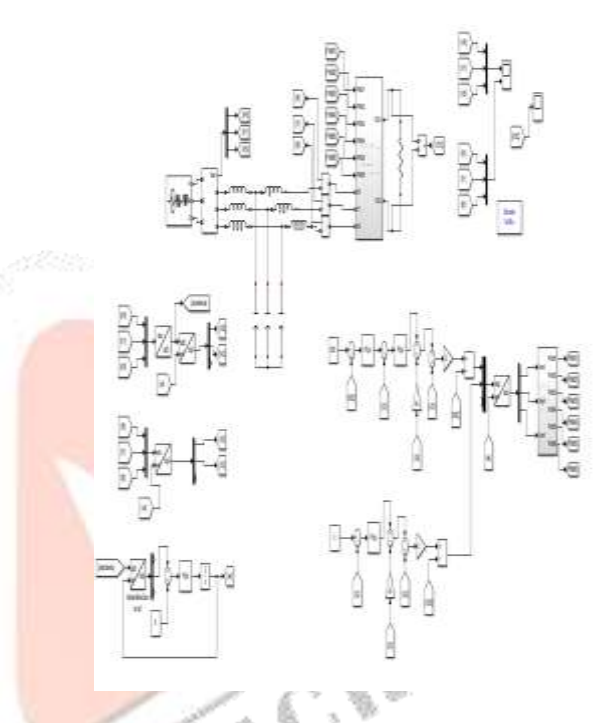


Fig. 2 the system in MATLAB Simulink

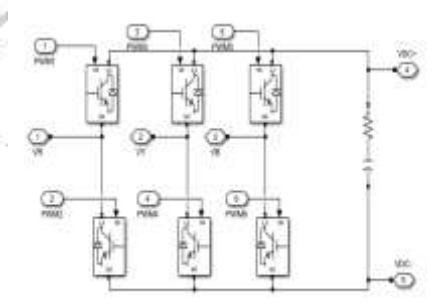


Fig. 3 Rectifier circuit

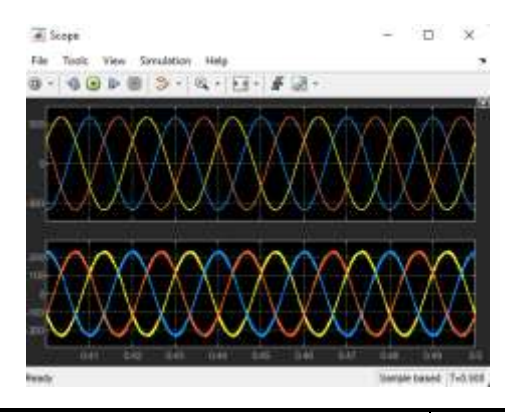


Fig. 4 The steady state voltage and current waveforms

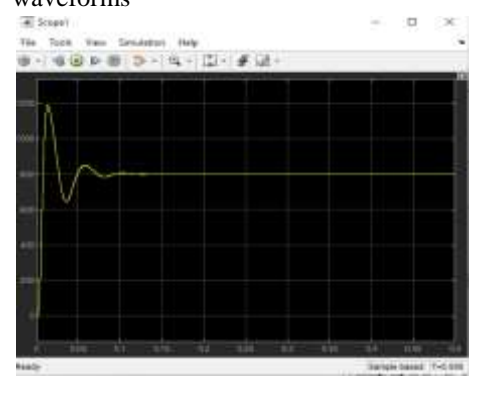


Fig. 5 The VDC output waveform

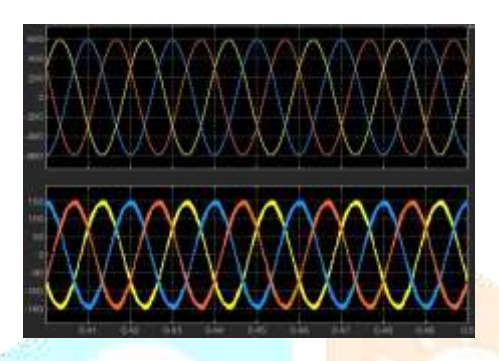


Fig. 6 The VI waveform when load is increased from 6.4 to 10 ohms



Fig. 7 the VDC output when load is increased from 6.4 to 10 ohms

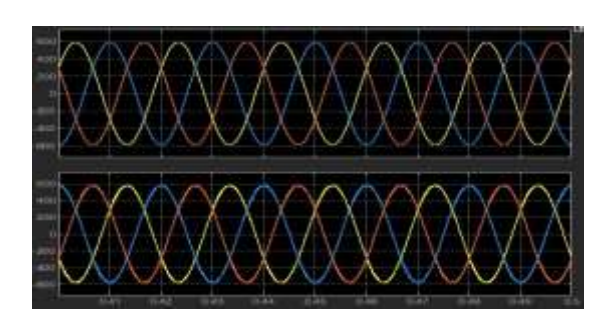


Fig. 8 VI waveforms when load is decreased from 6.4 to

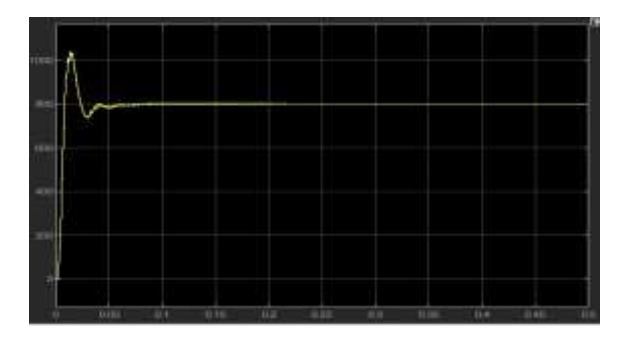


Fig. 9 VDC output voltage when load is decreased from 6.4 to 2.5

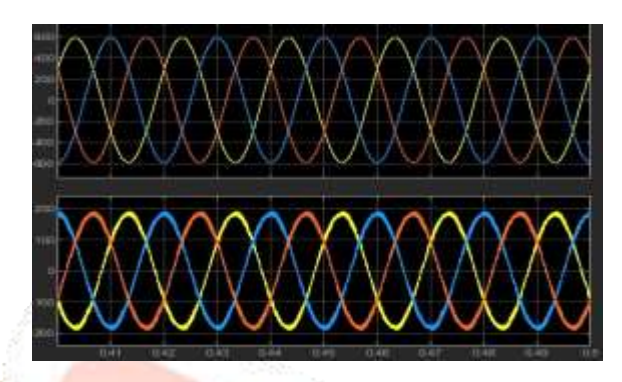


Fig. 10 the VI waveforms when dc link reference voltage is increased from 800 to 900

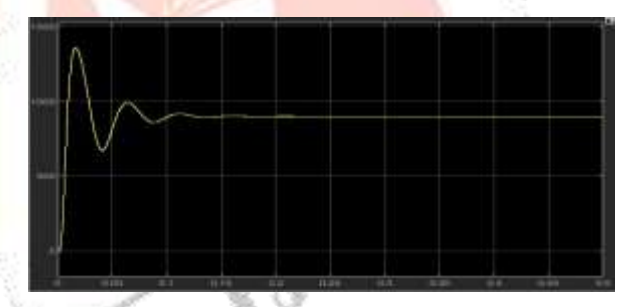


Fig. 11 the output voltage when dc link reference voltage is increased from 800 to 900

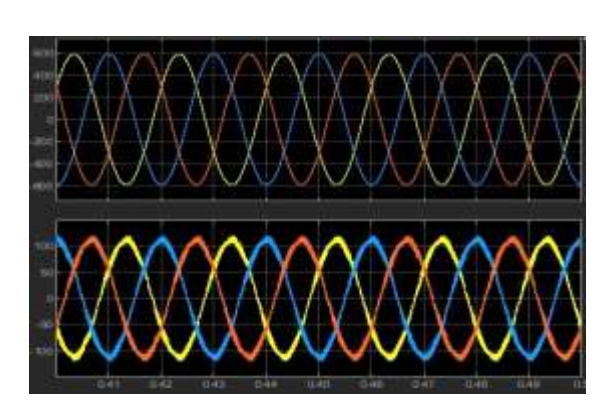


Fig. 12 the VI waveforms when dc link reference voltage is decreased from 800 to 700

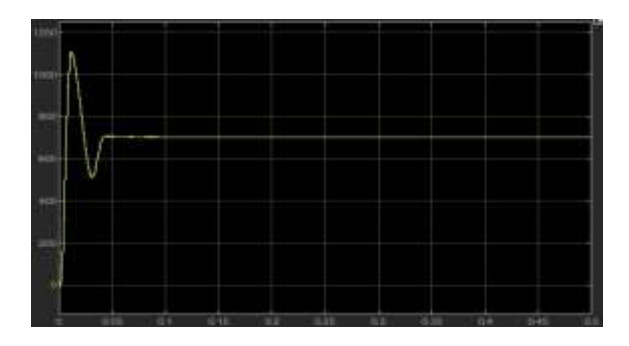


Fig. 13 the output voltage when dc link reference voltage is decreased from 800 to 700

As of the experimental results the figures (5), (6) show the steady state waveforms of the voltage and current of the system and the output dc voltage respectively. The sinusoidal waveforms of the current and voltage is been observed.

To validate the system more the dynamic response of the system for change of the load is been conducted for both increasing and decreasing of the load. The figure (7) shows the waveforms of voltage and current for increasing the load from 6.4 to 10 ohms, this increase of the load increases the voltage peak from 500 to 600 and subsequently decreases the current peaks from 200 to 150. The figure (8) shows the output waveform and it is seen that although the load is increased the output remains same which the desired result of the system. The figure (9) shows the VI waveforms of the system for a decreased load to 2.5 ohms, this cause current waveforms to increase it is peak to 600 and voltage to 600, but as of figure (10) the output dc voltage remains same and does not change which is a good result. It is seen that the system can with stand with dynamic change of the load and keeps the output same.

The system is also been tested by changing the dc reference for figure (11) shows the VI waveforms for increased reference voltage and figure (12) shows the output dc waveform which shows it is changed to the new reference voltage which 900. Figure (13) shows when the reference is decreased to 700 the voltage waveform remains same but the current waveform changes its peak. Figure (14) also shows the dc output voltage for the decreased reference voltage.

#### conclusion

This paper investigates the design and control of a three-phase active front-end rectifier using decoupled dg control. Decoupled dg control was designed based on a detailed mathematical model, to externally balance the generated active and reactive power. The implementation of the MATLAB/Simulink simulation system includes an LCL filter and a three-phase bridge inverter. The simulation results indicated that this control strategy could enable the system to working stably and efficiently in different ways. Although the

model complexity, parameter selection and practical implementation introduce more challenges for this approach to be used as a standard method in power electronics, it did provide reasonable results to build some insights about future research or industrial applications.

#### References:

- 1) Kazmierkowski, M. P., Franquelo, L. G., Rodriguez, J., Perez, M. A., Leon, J. I.: Highperformance motor drives. IEEE Ind. Electron. Mag. 5(3), 6–26,(2011).
- 2) Vazquez, S., Lukic, S.M., Galvan, E., Franquelo, L.G., Carrasco, J.M.: Energy storage systems for transport and grid applications. IEEE Trans. Ind. Electron. 57(12), 3881-3895 (2010).
- 3) Blaabjerg, F., Liserre, M., Ma, K.: Power electronics converters for wind turbine systems. IEEE Trans. Ind. Appl. 48(2), 708–719 (2012).
- Wang, P., Bi, Y., Gao, F., Song, T., Zhang, Y.: An improved deadbeat control method for singlephase PWM rectifiers in charging system for Evs. IEEE Trans. Veh. Technol. 68(10), 9672-9681 (2019).
- S. Bayhan and H. Komurcugil, "Sliding-mode control strategy for threephase three-level T-type rectifiers with DC capacitor voltage balancing," IEEE Access, vol. 8, pp. 64555-64564, 2020.
- 6) Komurcugil, H., Kukrer, O.: Lyapunov-based control for three-phase PWM AC/DC voltagesource converters. IEEE Trans. Power Electron. 13(5), 801–813 (1998).
- 7) Bouafia, A., Gaubert, J. P., Krim, F.: Predictive direct power control of three-phase pulsewidth modulation (PWM) rectifier using space-vector modulation (SVM). IEEE Trans. Power Electron. 25(1), 228–236 (2010).
- Tarisciotti, L., Zanchetta, P., Watson, A., Clare, J. C., Degano, M., Bifaretti, S.: Modulated model predictive control for a three-phase active rectifier. IEEE Trans. Ind. Appl. 51(2), 1610-1620 (2015).
- Zhong, Q. C., Konstantopoulos, G. C.: Currentlimiting three-phase rectifiers. IEEE Trans. Ind. Electron. 65(2), 957–967 (2018).
- 10) Rahoui, A., Bechouche, A., Seddiki, H., Abdeslam, D. O.: Grid voltages estimation for three-phase PWM rectifiers control without AC voltage sensors. IEEE Trans. Power Electron. 33(1), 859–875 (2018).
- 11) Trinh, Q. N., Wang, P., Choo, F. H.: An improved control strategy of three-phase PWM rectifiers under input voltage distortions and DC-offset measurement errors. IEEE J. Emerging Sel. Top. Power Electron. 5(3), 1164–1176 (2017).
- 12) Liserre, M., Aquila, A. D., Blaabjerg, F., Hansen, S.: Genetic algorithmbased design of the active damping for an LCL-filter three-phase active

- rectifier. IEEE Trans. Power Electron. 19(1), 76–86 (2004).
- 13) Liserre, M., Blaabjerg, F., Hansen, S.: Design and control of an LCL-filterbased three-phase active rectifier. IEEE Trans. Ind. Appl. 41(5), 1281– 1291 (2005).
- 14) Malinowski, M., Bernet, S.: A simple voltage sensorless active damping scheme for three-phase PWM converters with an LCL filter. IEEE Trans. Ind. Electron., 55(4), 1876–1880 (2008).
- 15) Milczarek, A., Mozdzynski, K., Malinowski, M., Stynski, S.: Effective and simple control of gridconnected three-phase converter operating at a strongly distorted voltage. IEEE Access 8, 12307– 12315 (2020).
- 16) Dannehl, J., Wessels, C., Fuchs, F. W.: Limitations of voltage-oriented PI current control of grid-connected PWM rectifiers with LCL filters. IEEE Trans. Ind. Electron. 56(2), 380–388 (2009).
- 17) Dannehl, J., Fuchs, F. W., Thogersen, P. B.: PI state space current control of grid-connected PWM converters with LCL filters. IEEE Trans. Power Electron. 25(9), 2320–2330 (2010).
- 18) Houari, A., Renaudineau, H., Martin, J. P., Mobarakeh, B. N., Pierfederici, S., Tabar, F. M.: Large-signal stabilization of AC grid supplying voltagesource converters with LCL-filters. IEEE Trans. Ind. Appl. 51(1), 702–711 (2015).
- 19) Falkowski, P., Sikorski, A.: Finite control set model predictive control for grid-connected AC-DC converters with LCL filter. IEEE Trans. Ind. Electron. 65(4), 2844–2852 (2018).
- 20) Chen, C., Xiong, J., Wan, Z., Lei, J., Zhang, K.: A time delay compensation method based on area equivalence for active damping of an LCL-type converter. IEEE Trans. Power Electron. 32(1), 762–772 (2017).
- 21) Said-Romdhane, M. B., Naouar, M. W., Slama-Belkhodja, I., Monmasson, E.: Robust active damping methods for LCL filter based grid connected converters. IEEE Trans. Power Electron. 32(9), 6739–6750 (2017).
- 22) Mora, D., Nunez, C., Visairo, N., Segundo, J., Camargo, E.: Control for three-phase LCL-filter PWM rectifier with BESS-oriented application. Energies, 12, 1–17 (2019).

- 23) Dian, R., Cai, X., & Li, C. (2023). Feed-Forward Control Strategy for Cascade H-bridge High-Voltage Inverter based on Active Front-end Rectifier. in \*Proc. 26th Int. Conf. Electrical Machines and Systems (ICEMS)\*, 2023, pp. 1-6, doi: 10.1109/ICEMS59686.2023.10344954.
- 24) Bayhan, S., & Komurcugil, H. (Year). A current sensorless control method for multi-level active front-end rectifiers with LCL filter. IET Power Electron. 2023;16:715–727.
- 25) Zhaksylyk, A., Rasool, H., Abramushkina, E. E., Chakraborty, S., Geury, T., Baghdadi, M. E., & Hegazy, O. (2023). Review of Active Front-End Rectifiers in EV DC Charging Applications. *Batteries* 2023, *9*(3), 150; doi.org/10.3390/batteries9030150
- 26) Ali, I. B., Naouar, M. W., & Monmasson, E. (2020). Design of an active front-end rectifier controller with an accurate estimation for the dynamic of its deadbeat current control loop. SN Appl. Sci. 2, 1054 (2020). doi.org/10.1007/s42452-020-2869-y.
- 27) Qin, N., & Ma, L. (Year). Disturbance Decoupling for a Single-Phase Pulse Width Modulation Rectifier Based on an Extended H-Infinity Filter, Computer laboratory for electrical systems, INSAT, University of Carthage, Centre Urbain Nord BP 676 – 1080.
- 28) Shi, C. (Year). Decoupling Control Strategy of DC Power Supply System Combining 24-pulse Rectifier and ISOP-DAB. IEEE conference in power systems and Electrical Technology, 10.1109/PSET56192.2022.10100473
- 29) Han, W., Li, X., Qin, C., Pang, X., & Zhang, C. (Year). Decoupling Control of Circulating Current Suppression and Current Distortion Elimination for the Paralleled Vienna-Type Rectifiers. IEEE Energy Conversion Congress and Exposition, 10.1109/ECCE50734.2022.9947685.
- 30) Bechir Bouaziz, Faouzi Bacha. Direct power decoupling control using optimal switching table combined with virtual flux estimator for PWM rectifier, 04 July 2023, PREPRINT (Version 1) available at Research Square [https://doi.org/10.21203/rs.3.rs-3130735/v1].